

Modelling and Simulation of the Logical Structure of Aircraft Power Distribution Systems

Xudong SHI *, Junchao QU, Huidong WU, Jin CAI, Zhangang YANG

College of Electronic Information and Automation, Civil Aviation University of China, Tianjin, 300300, China

Abstract — Increasingly more electrical devices are being developed in modern aircraft and will result in an increase in airborne electronic equipment fed by power electronic converters. With aircraft power system being sizable, the logical structure of aircraft power distribution systems, which affects the stability of aircraft power system, is becoming more complex. In this paper, we establish a mathematical model of the important modules of aircraft electrical power distribution system. Then the fault conditions are analyzed under a single generator failure and three-phase short circuit of transformer rectifier unit. The waveforms of voltage and current are analyzed to assess the logic operation of the power distribution system under fault conditions. It is demonstrated that the model and simulation of the components can be used to simulate the operation of electrical power distribution systems in different states.

Keywords - aircraft electrical power distribution system; logical structure; mathematical model; simulation.

I. INTRODUCTION

That many functions of the more-electronic aircraft managed by hydraulic, pneumatic and mechanical power are replaced by electronic power represents the development trend of the advanced aircraft. There are power system, power distribution system and load in aircraft power system. It plays a key role for airborne equipment to ensure reliable operation and ensure flight safety that power distribution systems defined by realizing electricity distribution, transmission, control, protection, and management from main bus to electric equipment, including DC-DC converters, DC-AC converters, AC-DC converters and other power electronic converters and harmonic compensation components.

It is obviously that the accurate modeling of aircraft power distribution system can be used to improve system design level, increase load capacity, restrain fluctuations of voltage and power, forecast and correct hazardous conditions. Computer simulation technology with high efficiency, high quality and economic characteristics, has good development prospects, applied in the theoretical research, technology development and evaluation on aircraft electrical system.

The state space model is established to realize the small disturbance analysis of system with AC/DC and driver loading [1]. The 270V high voltage distribution logical structure model of DC power system for a particular model of aircraft has been established by using LabVIEW to create a semi-physical simulation platform to simulate distribution network and conduct validation experiments [2]. In [3], by using Saber simulation software, the analyses and simulations are studied for the working principle and features of the main modules of secondary power supply system, such as transformer converter (AC/DC) and DC/AC inverter. The author has studied the AC/DC converter circuit of key components of more electric power system, also has

compared and analyzed the application of different AC/DC converter in more electric aircraft [4-5]. In order to study and simulate the fault diagnosis of aircraft power system, the State-space average method is used to establish the DQ model equation of inverter for aircraft electric power system [6]. According to the National Military Standards of power supply, it was tested that the simulation model to verify the protection for aircraft electrical power system under various fault conditions [7]. In [8], it is established that the model library of the more-electric aircraft (MEA) advanced power system various modules. According to the National Military Standards, it is demonstrated that the MATLAB/SIMULINK simulation model of a new type aircraft automatic power distribution system can be used to analyze the system characteristics in which the components are fault of over voltage, over frequency, under voltage, and under frequency etc. [9].

It can be easily seen that the state-space modeling and simulation of aircraft electrical power distribution system focused on a specific part of the aircraft electrical power distribution system. The overall logical structure simulation of distribution aircraft power distribution system is neglected. So, in this paper, the system composition and working principle of aircraft electrical power distribution system is analyzed. Then the logical structure simulation of aircraft generator distribution system is established to simulate the status of system under normal and emergency conditions and analyze the steady state and transient characteristics of system.

II. SYSTEM OVERVIEW

The AC power system of traditional CSCF (Constant Speed Constant Frequency) is adopted that in the Boeing 737 aircraft. Fig. 1 summarizes a top-level line diagram of this

power architecture. The main power is organized in two 90KVA constant speed constant frequency three-phase AC generators. Constant frequency generator is driven by integrated generator (IDG) to convert the main gear box of the motor speed into constant speed. Although the reliability, maintainability, weight, cost and other aspects of the CSCF power system has been the existence of different degrees of disadvantage, the CSCF power system is still widely adopted in the field of civil aviation aircraft at present. IDG1 and IDG2 which are controlled by generator control unit (GCU) output the 115V/400Hz three-phase alternating current to the AC bus which is connected to the transformer rectifier unit,

the emergency AC bus and other AC loads (de-icing and anti-icing units, kitchen, etc.). The 115V/400Hz three-phase AC is converted into 28V DC and then supplied to DC bus bar through the transformer rectifier unit. For the actual aircraft, Emergency AC bus which is connected with a battery through the converter supplies power to all flight critical equipment. For there is little effect on the performance of distribution system, in this paper, it is not taken into account and replaced by the electric actuator which is based on Permanent-magnet generator model that the battery and power electronic converters. DC bus bar is connected to resistance load and DC motor.

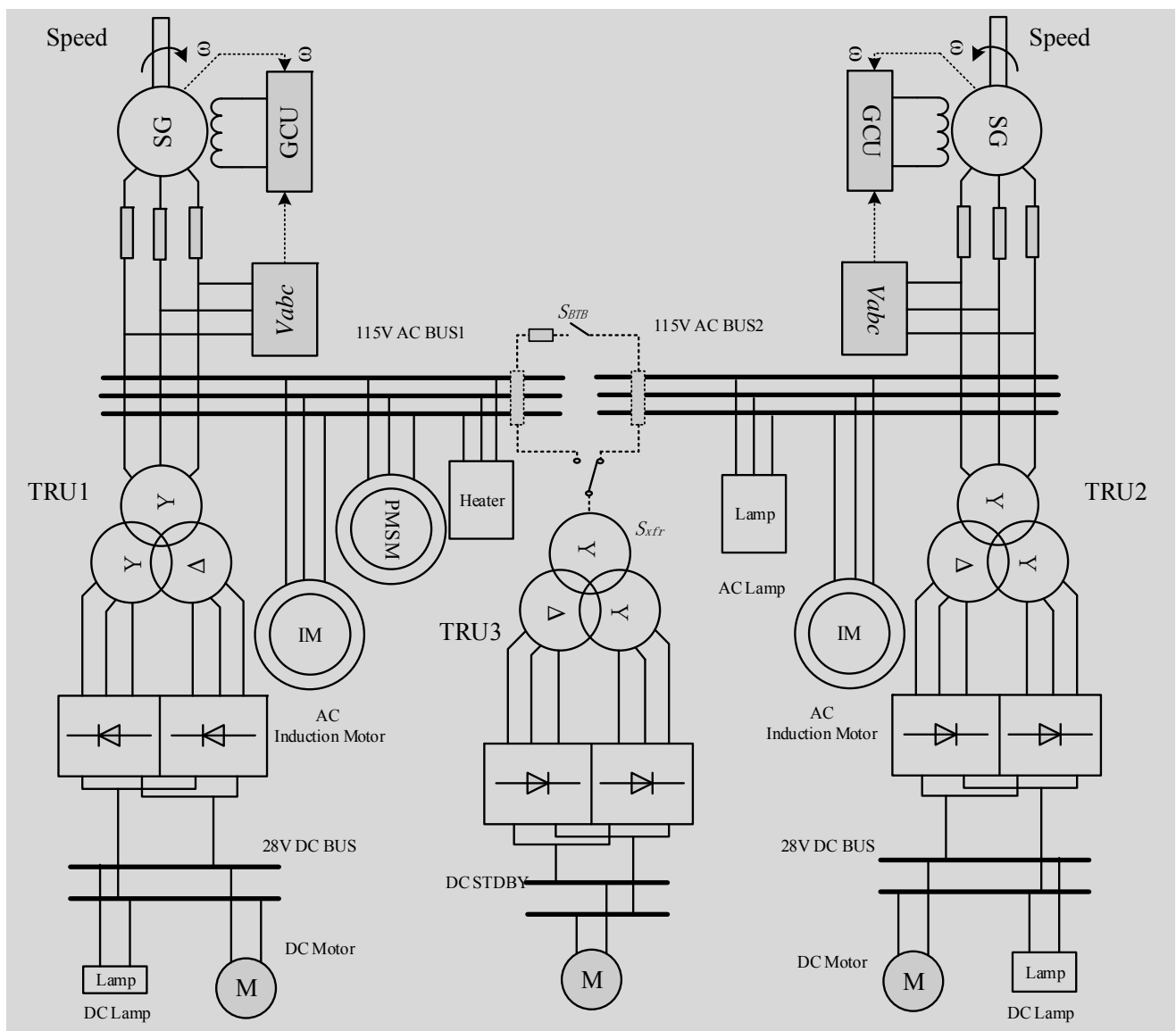


Figure. 1. Aircraft Distribution System Structure Diagram.

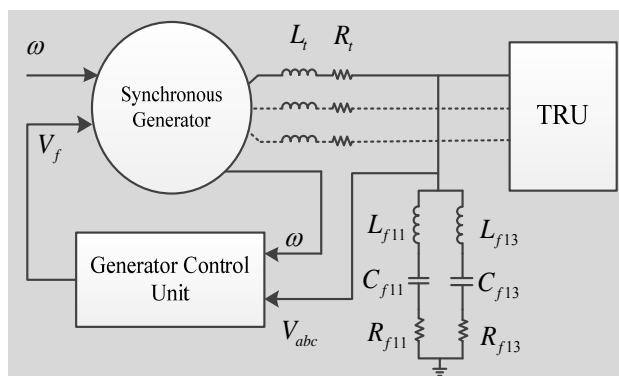
In this paper, the modeling of aircraft electrical power distribution system is focused on consists of the following

modules: synchronous generator under GCU control and transformer rectifier unit.

III. DYNAMIC MODELING OF AIRCRAFT GENERATOR

A. Synchronous Generator Modeling

In this section, the synchronous generators can generate the 90kVA 115V400Hz three-phase AC. The Fig. 2 shows the control structure of synchronous generator. The speed ω and excitation voltage V_f are two inputs of synchronous generator and the three-phase alternating current is output. The three-phase voltage of the output of the generator and the speed signal are collected through the sensor and transmitted to the GCU. Then the generator is controlled by GCU after analyzing excitation voltage of output.



FFigure2. Synchronous Generator Control Structure

The GCU is the key of synchronous generator control. It is expressed that the control functions of GCU by the formula (1) to the formula (6). The speed ω and the three-phase voltage V_{abc} are inputs, the excitation voltage V_f is output.

$$E_{fd} = \left(V_{ref} + V_{stab} + \frac{V_{f0}}{K_a} - V_{tf} - \frac{K_f s}{t_f s + 1} V_f \right) \frac{t_c s + 1}{t_b s + 1} \frac{K_a}{t_a s + 1} \quad (1)$$

$$V_f = \frac{(t_f s + 1)}{K_f s} (V_{ref} + V_{stab} - V_{tf}) - \frac{(t_a s + 1)(t_b s + 1)(t_f s + 1)}{K_a K_f (t_c s + 1)} E_{fd} \quad (2)$$

$$V_{tf} = \frac{1}{t_r s + 1} \sqrt{V_d^2 + V_q^2} \quad (3)$$

$$V_f = \frac{1}{t_e s + K_e} E_f \quad (4)$$

$$E_f = \begin{cases} E_{fd} & \text{when } E_{fd} > e_{f \min}, E_{fd} < u_1 \\ u_1 & \text{when } E_{fd} > e_{f \min}, E_{fd} \geq u_1 \\ e_{f \min} & \text{when } E_{fd} \leq e_{f \min}, E_{fd} < u_1 \\ e_{f \min} + u_1 & \text{when } E_{fd} \leq e_{f \min}, E_{fd} \geq u_1 \end{cases} \quad (5)$$

$$u_1 = \begin{cases} e_{f \max} & \text{when } k_p = 0 \\ k_p V_{tf} & \text{when } k_p \neq 0 \end{cases} \quad (6)$$

In formulas, V_{ref} is the reference voltage (p.u.), V_{stab} is the system stabilizer (p.u.); V_d is direct axis component of terminal voltage (p.u.), V_q is cross axis component (p.u.); V_f is excitation voltage (p.u.); K_f and t_f are the gain and time constant of damped filter (first order differential feedback); K_a and t_a are the gain and time constant of internal rectifier; K_e and t_e are the gain and time constant of excitation module; t_b, t_c are time constant of lead and lag compensation device; V_{tf} and K_p are output restrictions and gain of rectifier; V_{f0} and V_{f0} are initial value of terminal voltage and the excitation voltage.

As Fig. 3 shown, GCU control block diagram is simplified with specific parameters. The signal of three-phase and rotating speed is transformed into dq0 coordinates through park transformation. And in dq0 coordinates, the control of output of excitation voltage is realized. In this paper, V_{ref} is the reference voltage, per unit value is 1 and V_{stab} is equal to 0. The E_{fd} , V_{tf} and E_f are proportional saturation module to control the range of output.

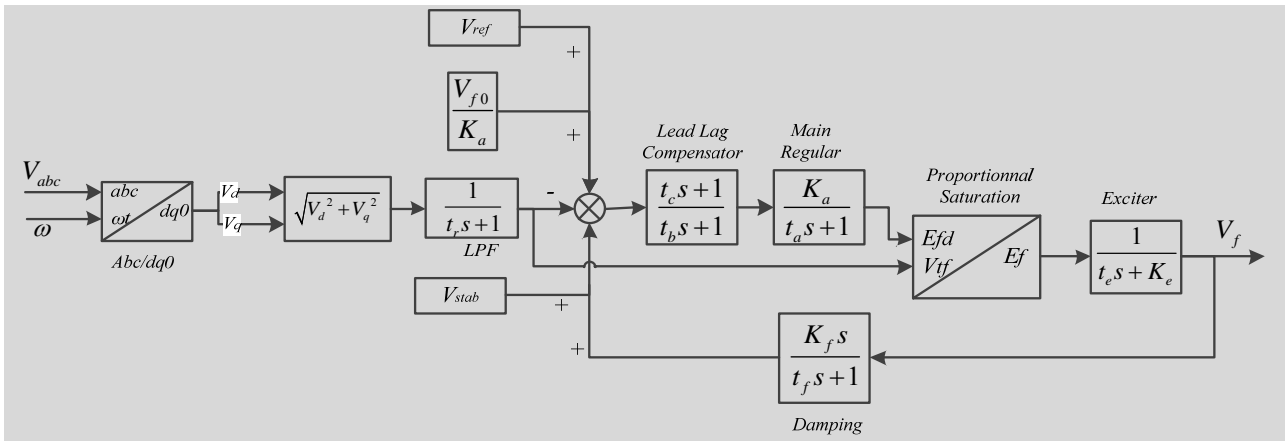


Figure3. Motor Control Unit Control Block Diagram.

B. Transformer Rectifier Unit Modeling

In this section, it is assumed that the current of the

variable voltage rectifier module ($I'_{gr}, I'_{gs}, I'_{gt}$) is continuous and full bridge rectifier diodes are ideal. In Fig. 4, a full bridge power supply with low pass filter is shown.

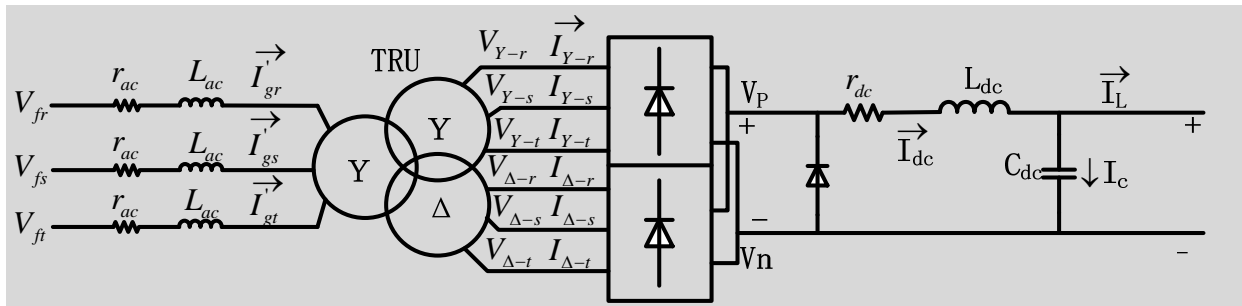


Figure 4. Transformer Rectifier Units.

In each cycle, the direction of the voltage and the current between the AC input side and DC link is simply converted through the diode bridge network of the rectifier unit. So the relationship between AC input and DC output can be considered as a naturally commutated full bridge rectifier diode. And the nonlinear equation is described as follows. Assuming overall conversion ratio of rectifier up and down bridge (according to the neutral point measurement) can be expressed as formula 7 and 8. V'_m is the peak phase voltage of band-pass filter.

$$\begin{cases} V_{Y-r} = V_{fr} = V'_m \sin\left(\omega t + \frac{\pi}{2}\right) \\ V_{\Delta-s} = V_{fs} = V'_m \sin\left(\omega t - \frac{\pi}{6}\right) \\ V_{\Delta-r} = V_{ft} = V'_m \sin\left(\omega t - \frac{5\pi}{6}\right) \end{cases} \quad (7)$$

$$\begin{cases} V_{\Delta-r} = V'_m \sin\left(\omega t + \frac{\pi}{2} + \frac{\pi}{6}\right) = V'_m \sin\left(\omega t + \frac{\pi}{3}\right) \\ V_{\Delta-s} = V'_m \sin\left(\omega t - \frac{\pi}{6} + \frac{\pi}{6}\right) = V'_m \sin(\omega t) \\ V_{\Delta-r} = V'_m \sin\left(\omega t - \frac{5\pi}{6} + \frac{\pi}{6}\right) = V'_m \sin\left(\omega t - \frac{2\pi}{3}\right) \end{cases} \quad (8)$$

In a power system with a power rating of 90kW, the DC load current is relatively low. So commutation angle μ may be considered less than $\pi/6$ and the commutation interval in the upper and lower bridge does not overlap. Then the continuous state of DC bus bar can be expressed as nonlinear equation (9, 10).

$$\begin{aligned} V_{dc} + R_2 C_{dc} \frac{dV_{dc}}{dt} + L_2 C_{dc} \frac{d^2 V_{dc}}{dt^2} &= \frac{6 + 3\sqrt{3}}{7} V'_m \sin\left(\theta + \frac{2\pi}{3}\right) - R_2 I_L - L_2 \frac{dI_L}{dt} \\ -\frac{\pi}{4} &\leq \theta < \mu - \frac{\pi}{4} \end{aligned} \quad (9)$$

$$V_{dc} + R_2 C_{dc} \frac{dV_{dc}}{dt} + L_2 C_{dc} \frac{d^2 V_{dc}}{dt^2} = \frac{1}{2} \left\{ \sqrt{3} V_m \sin\left(\theta + \frac{\pi}{2}\right) + \sqrt{3} V_m \sin\left(\theta + \frac{2\pi}{3}\right) \right\} - R_2 I_L - L_2 \frac{dI_L}{dt}, \mu - \frac{\pi}{4} \leq \theta < -\frac{\pi}{12}$$
(10)

$$R_1 = r_{dc} + \frac{6}{7} r_{ac}$$
(11)

$$L_1 = L_{dc} + \frac{6}{7} L_{ac}$$
(12)

$$R_2 = r_{dc} + r_{ac}$$
(13)

$$L_2 = L_{dc} + L_{ac}$$
(14)

In order to further simplify, equation (9) and (10) can be combined into (15).

$$L_2 C \frac{d^2 V_{dc}}{dt^2} + R_2 C \frac{dV_{dc}}{dt} + V_{dc} = - \left(R_2 I_L + L_2 \frac{dI_L}{dt} \right) + h(\theta, \mu) \frac{6 + 3\sqrt{3}}{7} V_m \sin\left(\theta + \frac{2\pi}{3}\right) + (1 - h(\theta, \mu)) \frac{1}{2} \left\{ \sqrt{3} V_m \cos(\theta) + \sqrt{3} V_m \sin\left(\theta + \frac{2\pi}{3}\right) \right\}$$
(15)

Here, the commutation function is defined by

$$h(\theta, \mu) = \begin{cases} 1 & , \quad 2n\pi - \frac{\pi}{4} \leq \theta < 2n\pi + \mu - \frac{\pi}{4} \\ 0 & , \quad 2n\pi + \mu - \frac{\pi}{4} \leq \theta < 2n\pi - \frac{\pi}{12} \end{cases}$$
(16)

Where n is an integer and cycle of periodic function $h(\theta, \mu)$ is $\pi/6$. In addition, differential equation of state space expression (15) can be described by

$$\begin{bmatrix} \dot{X}_v \\ \dot{X}_c \end{bmatrix} = \begin{bmatrix} 0 & \frac{1}{C} \\ -\frac{1}{L_2} & -\frac{R_2}{L_2} \end{bmatrix} \begin{bmatrix} X_v \\ X_c \end{bmatrix} + \begin{bmatrix} -\frac{1}{C} & 0 \\ 0 & \frac{1}{L_2} \end{bmatrix} \begin{bmatrix} I_L \\ f_v \end{bmatrix}$$
(17)

Where the filter capacitor voltage $X_v = V_{dc}$ and the DC link voltage $X_c = I_{dc}$ is selected as the state variables. The f_v can be expressed by

$$f_v = f_v(V_m, \theta, \mu) = h(\theta, \mu) \frac{6 + 3\sqrt{3}}{7} V_m \sin\left(\theta + \frac{2\pi}{3}\right) + (1 - h(\theta, \mu)) \frac{\sqrt{3}}{2} \left\{ V_m \cos(\theta) + V_m \sin\left(\theta + \frac{2\pi}{3}\right) \right\}$$
(18)

C . Modeling and Simulation of Single Generator

In this section, the circuit simulation model of single generator is established. As Fig. 5 shown, the structure is organized in 4 parts: the first part is the power generator module which is driven by rotating speed signal and whose rated power is 50KW. GCU collects three phase voltage signals and rotating speed signals to control the line voltage of the generator in 200V; The second part is 115V/400Hz AC bus and AC load which mainly consists of 12kW induction motor, 1KW resistive load (electric lamp) and 3 HP permanent magnet synchronous motor; The third part is the transformer rectifier module which converts 115V AC to 28V DC; The DC load which mainly include resistive load (electric light and electric heater) and DC motor with 300 power which can drive the fuel pump are contained in the fourth part.

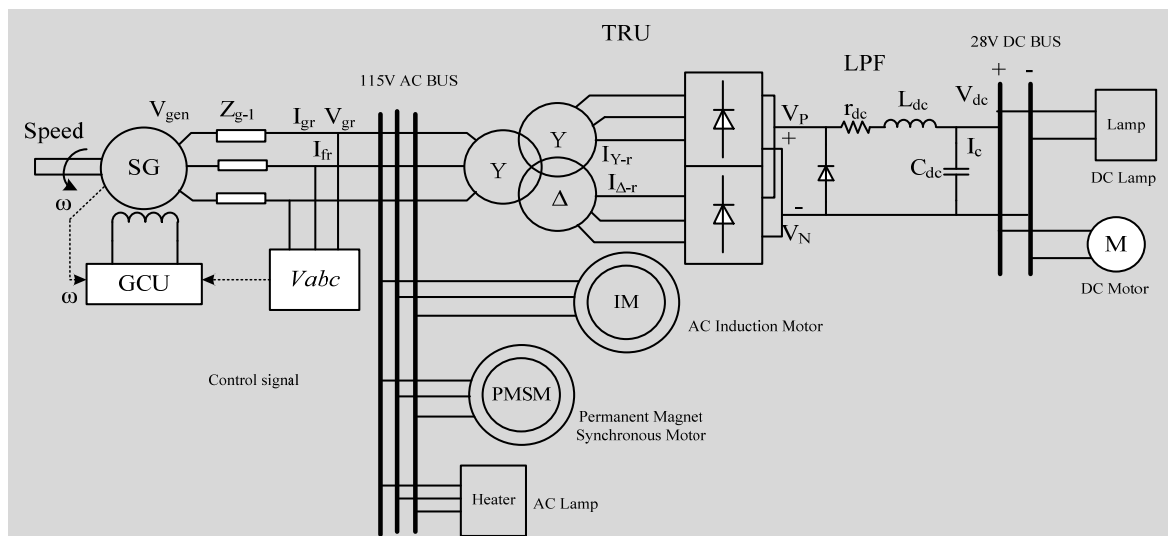


Figure 5. Branch Circuit Structure of Single Generator.

In Fig. 6, simulation results of generator output is shown. Fig. 6 (a) represents the voltage waveform, the voltage peak is 282V and the frequency is 400Hz. Fig. 6 (b) represents the current waveform, in 0.3 seconds, the generator rotating speed is reached the rated speed. The main switch is activated and the current is connected to the AC bus bar from the generator, so the current is zero until 0.3 seconds.

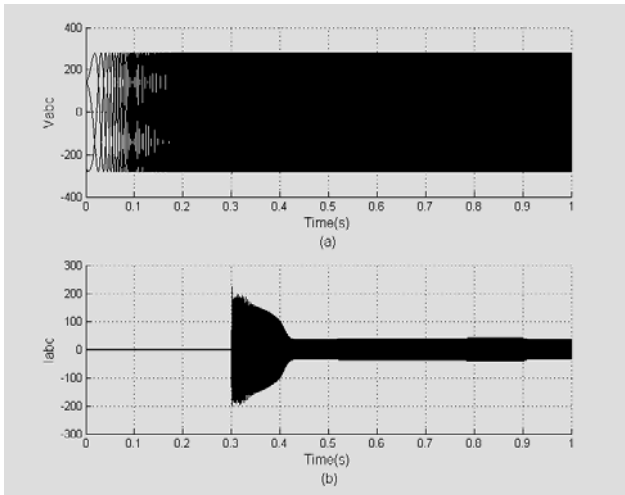


Figure 6. Generator Simulation Waveform.

The Fig. 7(a) shows the voltage waveform and (b) the current waveform. As the figure shown, change occurs at $t=0.3s$. The voltage steadies at 28V and current at 69A at $t=0.5s$.

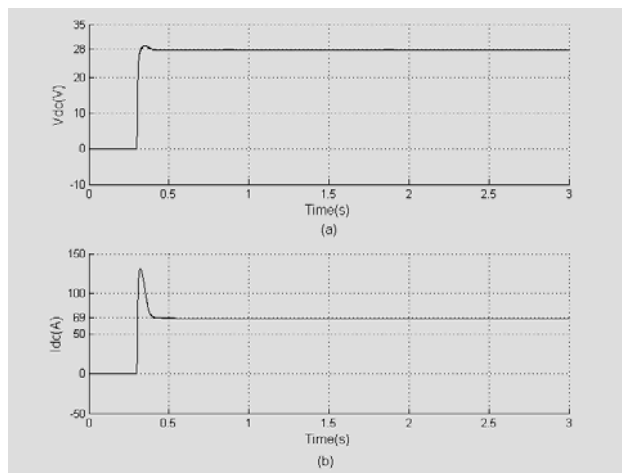


Figure 7. Simulation Waveform of 28V DC bus

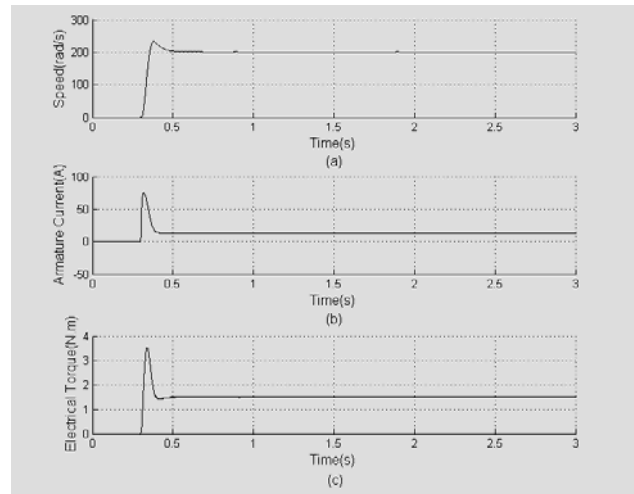


Figure 8. Simulation Waveform of brushed DC Motor.

Fig. 8 shows the simulation waveform of DC load with brushed DC motor as an example. The speed of motor reported in Fig. 8(a) reaches the rated speed 200rad/s at $t=0.5s$. The armature current shown in Fig. 8(b) reaches 75.5A in peak and 13A in steady. Fig. 8(c) shows the electromagnetic torque whose value of peak is 3.5N.m and value of steady is 1.5 N.m.

Fig. 9 shows simulation waveform of AC load with induction motor as an example. The speed of motor shown in Fig. 9(a) reaches the rated speed 300rad/s at $t=0.5s$. The armature current reported in Fig. 9(b) reaches 200A in peak and 23A in steady. Fig. 9(c) shows the electromagnetic torque whose value of peak is 100N.m and value of steady is 17N.m.

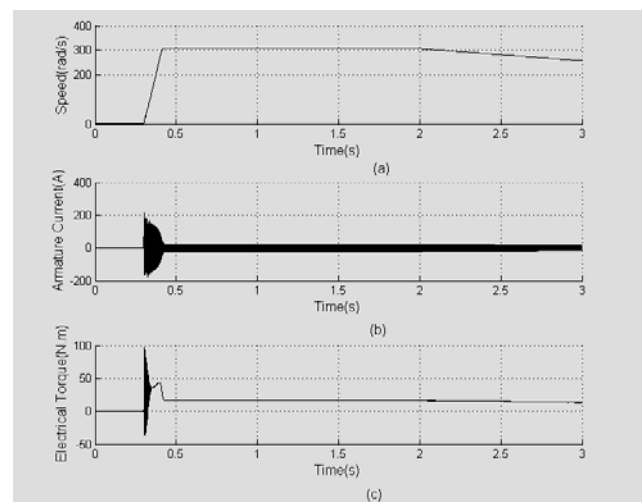


Figure 9. Simulation Waveform of Induction Motor.

IV. SYSTEM SIMULATION UNDER NORMAL CONDITIONS

For 737 power distribution systems, the AC system is organized in four sections: the integrate drive generator 1 (IDG1), the integrate drive generator 2 (IDG2), the auxiliary power unit (APU) starter generator and external power supply (EXT PWR). There is not power automatic collection when using cockpit switch to operate the power supply. Left and right parts of AC power system are independent power supplies (non-parallel power supply). The two power supplies will not supply power to the AC exchange transfer bus (XFR BUS) at the same time. If there is only one power supply (the left or right transfer bus lose the power and the external power supply or APU generator is the only power supply), the two parts of AC system will be combined.

The DC power equipment is supplied DC power by the transformer rectifier unit (TRU) through which AC is converted to DC. Firstly, the AC XFR BUS 1 is provided power by IDG1 which is controlled by GCU1, then the TRU1 is provided AC power by the AC XFR BUS 1, the same to the TRU2 by the AC XFR BUS 2. Usually the TRU3 is provided AC by the AC XFR BUS 2. If the switching relay of the TRU3 (S_{xfr}) is switched on when the AC XFR BUS 2 is switched off, the TRU3 will be provided AC from the AC XFR BUS 1. The continuous power supply provided by Each IDG is 90kVA and the same to external power adapter. Below 9753 meters, the power supply provided by APU starter generator is 90KVA and up to 12500 meters, the power will decline to 66kVA.

Fig. 1 shows the distribution structure of general power distribution system. In the case of normal state, the structure consists of three branches: TRU1, TRU2 and TRU3. It is assumed that the rated voltage frequency of output of synchronous generator is 400Hz, the apparent power of AC induction motor is 10KVA and the output power of brushed motor with DC load is 2KW. Fig. 10 shows the simulation waveform of AC bus 1. At $t=0.5s$, generator works normally and AC induction motor is connected. RMS value of line voltage is raised from 0 to 200V and RMS value of current from 0 to 135A. At $t=0.7s$, motor operates normally and current is steadies in 50A.

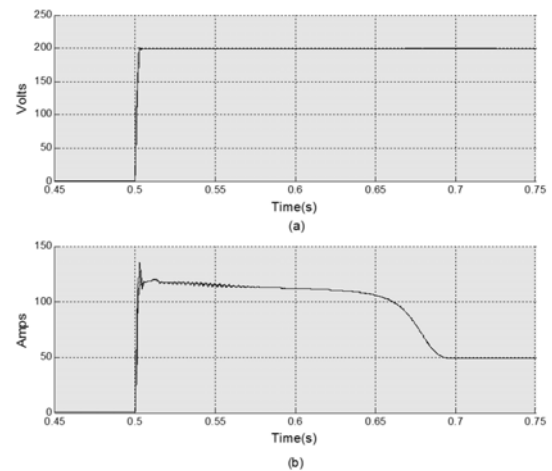


Figure 10. Simulation Waveform of AC Bus.

The simulation waveform of DC bus 1 is shown in Fig. 11. At $t=0.5s$, generator works normally and DC load (DC brushed motor and lamp) is connected. Fig. 11 shows that the peak value of current reached 75A. Motor starts up, and the current is stable at 13A at $t=0.6s$. Throughout the starting process, the voltage of DC bus 1 is stable at 28V.

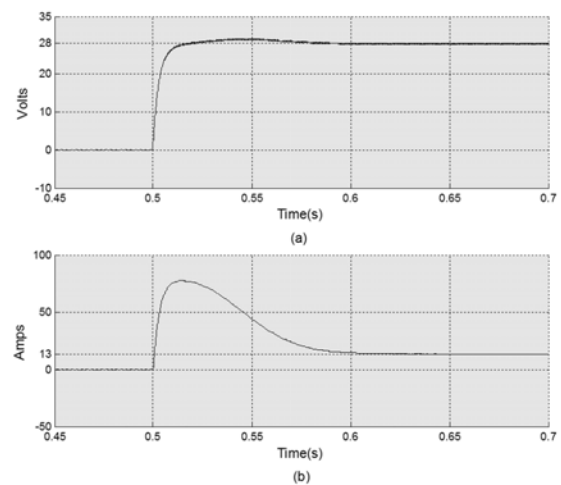


Figure11. Simulation of DC Bus.

V. SIMULATION OF POWER DISTRIBUTION SYSTEM UNDER NON-NORMAL CONDITION

For the aircraft power distribution system, it is an important rating indicator that the system can ensure safety of aircraft under critical condition. In this paper, based on two kinds of common faults, the simulation is carried out, which are single generator failure and three-phase short circuit.

A. Power Distribution System Simulation with A Single Generator Failure

The fault between synchronous generator (SG) 1 and AC

bus leads to failure of single generator is assumed. At $t=1s$, because that S_{BTB} is switched on according to control logic, SG 2 supplies electric energy to AC bus 1. In order to simulate the most urgent situation, it is assumed that all loads work at full power. Parts of flight critical loads will be deactivated or be in a low power state to ensure the running of the flight critical equipment under the fault condition. As Fig. 12 shown, at $t=1s$, there appear spikes about the voltage waveform, but quickly disappear. Then the voltage returns to the normal peak at 282V. As a result of unloading loads, there appear spikes at $t=1.02s$. Before the failure occurs, it is stable at 35A that the current waveform peak value of the AC bus bar 1. Then, after the failure occurs, the peak value of the current rapidly ascends to 75A. But, due to the protection mechanism of the distribution system, with unloading parts of non-essential electrical equipment, the peak value steadies at 55A after 20ms. In Fig. 13, the root mean square (RMS) value of current and voltage are shown. The changes of failure can be more intuitively expressed that the value of current rises from 25A to 35A and returns to 40A due to the unloading parts of loads.

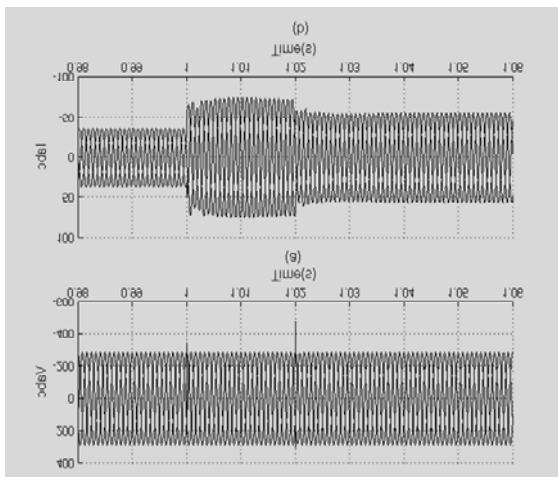


Figure 12. Simulation Waveform of Failure of Single Generator.

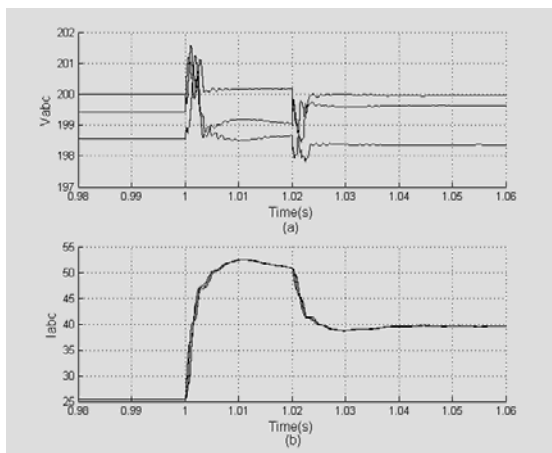


Figure 13. Simulation of RMS of Failure of Single Generator

B. Power Distribution System Simulation with The Three-Phase Short Circuit Of Transformer Rectifier Unit

In this paper, it is assumed that the three-phase short circuit (connected with small resistance) occurs between AC bus and TRU1. At $t=1s$, the A and B phase are connected with a 0.00001 resistor to form a short circuit fault. Short circuit fault is detected within 20ms and TRU1 branch is removed. Fig. 14 and Fig. 15 show the result of simulation. In Fig. 14, as a result of the fault, the voltage mutation that the line voltage between a-phase and b-phase becomes little, approximately 0 and the voltage peak value between c phase and a phase rises to 400V. The fault is detected within 20ms and removed automatically so that the voltage returns to normal after 0.05 seconds. The AC bus current rapidly rises to 1500A in one second. In Fig.15, the current RMS of a phase and b phase is 800A and the c phase is no more than 10A. After fault is removed automatically, the current returns to normal in 0.005s.

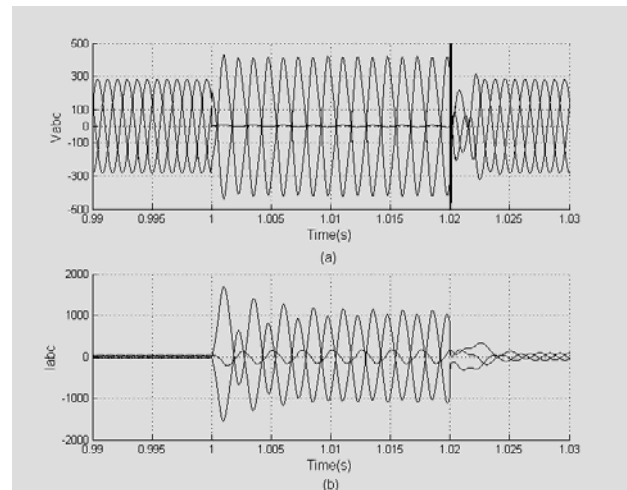


Figure 14. Waveform of Voltage and Current of AC Bus 1.

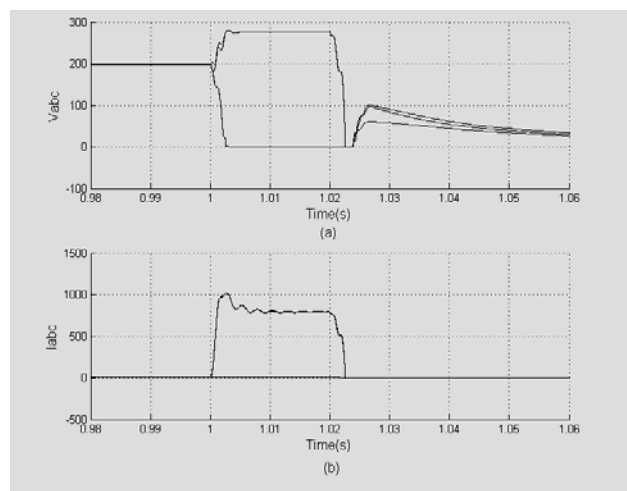


Figure 15. RMS of Current of AC Bus 1.

VI. CONCLUSION

In this paper, firstly, the distribution system is introduced. Then the composition and distribution logic of the aircraft electrical power distribution system are analyzed. Lastly, it is completed that the modeling of synchronous generator and transformer rectifier and the Simulink simulation of a single generator branch.

Based on modeling and simulation of components, a complete simulation model of distribution system is set up to simulate the running condition in normal state and abnormal state to analyze the simulation data. Based on model of synchronous generator, transformer rectifier and a variety of load, varieties of aircraft power distribution system simulation models can be built to realize more types of simulation and get more data in the future.

ACKNOWLEDGEMENTS

The authors thank the reviewers who gave a through and careful reading to the original manuscript. Their comments are greatly appreciated and have help to improve the quality of this paper. This work is supported in part by the National Natural Science Foundation of China (No.51377161, No.51407185) and the Fundamental Research Funds for The Central Universities (No.3122015D013).

REFERENCES

- [1] Weihua Chen. Research on the structure and simulation technique for aircraft 270V HVDC power supply system [D]. Nanjing : Nanjing University of Aeronautics and Astronautics, 2010.
- [2] Zhang Wei, Shang Xiaolei, Zhou Yuanjun, et al. A maximum power control method of three-phase voltage source rectifiers adapted to aircraft electric actuator load[J]. Diangong Jishu Xuebao (Transactions of China Electro technical Society), 2011, 26(8): 91-98.
- [3] Xu Gang. The Saber of aircraft power supply system simulation [D]. Xi'an: Northwestern Polytechnical University (NWPU), 2007.
- [4] Ni Jingmeng, Fang Yu, Xing Yan, et al. Three-phase 400Hz PWM rectifier based on optimized feedforward control for aeronautical application[J]. Transactions of China Electrotechnical Society, 2011, 26(2): 141-146.
- [5] Chensong Li. Study on the application of three-phase PWM rectifier in aviation[D]. Nanjing: Nanjing University of Aeronautics and Astronautics, 2012.
- [6] HUANG Jian, ZHANG Zhen. Stability of aircraft power supply system with constant power loads[J]. Transactions of China Electrotechnical Society, 2011, 26, (1): 213-318.
- [7] Shuanwei Ma, Shanshui Yang, Hong Li. Modeling and simulation of automatic power distribution system[C]. Shenzhen, China. The Sixteenth Annual Meeting of the national power technology of China Power Institute, 2005, 11: 539-542.
- [8] S. V. Bozhko, T. Wu, Y. Tao, G. M. Asher. More-electric Aircraft Electrical Power System Accelerated Functional Modeling[C]. Ohrid, Power Electronics and Motion Control Conference, 2010: T9. 7-T9. 14
- [9] Shuanwei Ma, Shanshui Yang, Hong Li. Modeling and simulation of aircraft automatic distribution system[J]. Journal of Nan jing University of Aeronautics & Astronautics, 2006, 38(4): 519-523.
- [10] FENG Jianzhao, REN Renliang, ZHAO Zunquan. Research of civil aircraft power distribution system[J]. Measurement & Control Technology, 2012, 31(12): 108-111.
- [11] Eid A, El-Kishky H, Abdel-Salam M, et al. Modeling and characterization of an aircraft electric power system with a fuel cell-equipped APU connected at HVDC bus[C]//Power Modulator and High Voltage Conference (IPMHVC), 2010 IEEE International. IEEE, 2010: 639-642.
- [12] Wu T, Bozhko S V, Asher G M. High speed modeling approach of aircraft electrical power systems under both normal and abnormal scenarios[C]//Industrial Electronics (ISIE), 2010 IEEE International Symposium on. IEEE, 2010: 870-877.
- [13] Dehong Xu. Modeling and control of power electronic system[M]. Machinery Industry Press, 2005. 40-43.
- [14] Dong Fengbin, Zhong Yanru. Exact linearization control of three-phase voltage source inverter[J]. Transactions of China Electrotechnical Society, 2013, 28(10): 143-149.